Removal of BRCA1/CtIP/ZBRK1 repressor complex on *ANG1* promoter leads to accelerated mammary tumor growth contributed by prominent vasculature

Saori Furuta,[1,2] Ju-Ming Wang,[1,2] Shuanzeng Wei,[1] Yung-Ming Jeng,[1] Xianzhi Jiang,[1] Bingnan Gu,[1]
Phang-Lang Chen,[1] Eva Y.-H.P. Lee,[1] and Wen-Hwa Lee[1,*]

[1] Department of Biological Chemistry, College of Medicine, University of California, Irvine, Irvine, California 92697
[2] These authors contributed equally to this work.
*Correspondence: whlee@uci.edu

Summary

BRCA1 exerts transcriptional repression through interaction with CtIP in the C-terminal BRCT domain and ZBRK1 in the central domain. A dozen genes, including angiopoietin-1 (*ANG1*), a secreted angiogenic factor, are corepressed by BRCA1 and CtIP based on microarray analysis of mammary epithelial cells in 3D culture. BRCA1, CtIP, and ZBRK1 form a complex that coordinately represses ANG1 expression via a ZBRK1 recognition site in the *ANG1* promoter. Impairment of this complex upregulates ANG1, which stabilizes endothelial cells that form a capillary-like network structure. Consistently, *Brca1*-deficient mouse mammary tumors exhibit accelerated growth, pronounced vascularization, and overexpressed ANG1. These results suggest that, besides its role in maintaining genomic stability, BRCA1 directly regulates the expression of angiogenic factors to modulate the tumor microenvironment.

Introduction

Mutations in the breast cancer susceptibility gene *BRCA1* account for up to 50% of hereditary breast cancer and for almost all cases of hereditary breast and ovarian cancer syndrome (Couch et al., 1997; Easton et al., 1993). Also, reduced *BRCA1* expression is often correlated with accelerated progression and growth of sporadic breast cancer (Thompson et al., 1995). BRCA1 participates in DNA damage repair, cell cycle checkpoint control, and transcriptional regulation, serving as a tumor suppressor to maintain genomic stability. The *BRCA1* gene encodes a 220 kDa nuclear phosphoprotein of 1863 amino acids (Chen et al., 1996; Miki et al., 1994), characterized by distinctive protein-protein interaction surfaces. The N-terminal RING finger domain dimerizes with BARD1 for ubiquitin ligase activity (Hashizume et al., 2001), while the C terminus possesses two tandem copies of the BRCT motif that interact with several cellular proteins, including CtIP (Li et al., 1999; Zheng et al., 2000a). The central region, mainly encoded by exon 11, contains two nuclear localization signals (Chen et al., 1995) and interacts with a DNA damage repair complex, Rad50/Mre11/NBS1 (Zhong et al., 1999), and transcription repressor, ZBRK1 (Zheng et al., 2000b).

BRCA1 is also involved in developmental and differentiation processes and exhibits a temporal and spatial expression pattern (Furuta et al., 2005; Lane et al., 1995). Developmental defects and early embryonic death (E6.5) are observed in *Brca1* homozygous knockout mice (Hakem et al., 1996; Liu et al., 1996). BRCA1 facilitates differentiation of mammary epithelia and is upregulated in rapidly dividing, differentiating cells (Marquis et al., 1995), whereas its depletion impairs differentiation and promotes cellular proliferation (Furuta et al., 2005). Consistently, in mouse mammary tissue a conditional *Brca1* knockout displays abnormal ductal morphogenesis and mammary tumor (Xu et al., 1999).

BRCA1 confers a transcriptional repression on stress-responsive genes *p21* and *GADD45* through interaction with CtIP at the C-terminal BRCT domain (aa 1651–1863) (Li et al., 1999, 2001; Yu et al., 1998). CtIP is an 897 amino acid protein that was originally identified as a cofactor of CtBP, a C-terminal binding protein of human adenovirus E1A protein, and is involved in transcriptional repression (Chinnadurai, 2006). CtIP interacts with different proteins via discrete modules, including a PLDLS motif (aa 490–494) for CtBP (Schaeper et al., 1998), a region aa 299–345, phosphorylated at S327, for BRCA1 (Yu and Chen, 2004), and a LECEE motif (aa 153–157) for retinoblastoma (RB) tumor

SIGNIFICANCE

BRCA1 plays an essential role in DNA damage response and cell cycle checkpoint control. Little is known about how an impaired function of BRCA1 is correlated with accelerated growth and progression of hereditary and sporadic breast cancer. We show that BRCA1 forms a repressor complex with CtIP and ZBRK1 at a ZBRK1-responsive element of the angiopoietin-1 promoter in mammary epithelial cells. A defect of this complex formation derepresses ANG1 transcription, promoting endothelial cell survival and vascular enlargement in a paracrine fashion. This enhanced angiogenesis contributes to exacerbated malignancy of *Brca1*-deficient mouse mammary tumors. Thus, our study unveils a mechanism for how BRCA1 modulates the tumor microenvironment by transcriptional regulation.

DOI 10.1016/j.ccr.2006.05.022

Table 1. Genes corepressed by BRCA1 and CtIP in 3D cultured MCF10A cells

		BRCA1-KD		CtIP-KD	
Gene symbol	Gene name	fold	p value	fold	p value
ACTR1A	ARP1 actin-related protein 1 homolog A, centractin α	+2.08	0.048	+2.09	0.047
ANG1*	angiopoietin-1	+2.69	0.016	+2.18	0.026
DCP2	decapping enzyme hDcp2	+2.19	0.027	+2.09	0.011
DRLM	downregulated in liver malignancy	+2.10	0.001	+2.00	0.008
FGF2*	fibroblast growth factor 2 (basic; bFGF)	+2.03	0.048	+2.04	0.008
HMGA2*	high mobility group AT-hook 2	+4.55	0.002	+2.55	0.001
IL1R1	interleukin 1 receptor, type I	+2.02	0.004	+2.09	0.001
LIMK1*	LIM domain kinase 1	+2.12	0.049	+2.06	0.005
RFC1*	replication factor C (activator 1) 1, 145kDa	+2.07	0.047	+2.07	0.027
SLC16A4	solute carrier family 16 (monocarboxylic acid transporters), member 4	+2.63	0.002	+2.21	0.037
TA-KRP	T cell activation kelch repeat protein	+2.17	0.048	+2.17	0.009

*Confirmed by RT-PCR (Figure S1).

suppressor (Fusco et al., 1998). Certain tumor-linked mutations of the BRCT domain abolish CtIP association and prevent BRCA1-dependent transcriptional repression (Li et al., 1999; Yu et al., 1998). Moreover, *Ctip* null mouse embryos die at E4.0 as blastocysts fail in S phase entry, while the heterozygotes are short-lived and develop various kinds of tumors that retain a single wild-type (wt) allele, indicative of haploid insufficiency, suggesting that *Ctip* is a bona fide tumor susceptibility gene (Chen et al., 2005).

Two interacting tumor suppressors, BRCA1 and CtIP, coordinate in certain transcriptional regulatory pathways, namely, DNA damage response and cell cycle checkpoint control (Li et al., 1999, 2001). However, it is largely unknown whether they cooperate in a transcriptional repression beyond the stress-inducible pathways. In the present study, we have identified a dozen genes corepressed by BRCA1 and CtIP in MCF10A mammary epithelial cells (MECs) in 3D culture using microarray analyses. Among them, we have examined angiopoietin-1 (*ANG1*), a factor secreted to stimulate angiogenesis of neighboring endothelial cells (Suri et al., 1996), for a BRCA1- and CtIP-dependent transcriptional repression. We demonstrate that BRCA1, CtIP, and ZBRK1 form a repressor complex at a recognition site of ZBRK1 in *ANG1* promoter, and a defect of this repressor complex formation derepresses ANG1 expression in MECs that promotes survival of the neighboring endothelial cells to form a capillary-like structure. Consistently, *Brca1*-deficient mouse mammary tumors display a high level of Ang1 expression, prominent vascularization, and accelerated growth.

Results

ANG1 expression is corepressed by BRCA1 and CtIP in MECs

We previously demonstrated that MECs depleted of BRCA1 in 3D matrix, a close mimicry to the in vivo microenvironment, undergo vigorous proliferation but fail in acinar differentiation (Furuta et al., 2005), reflecting a phenotype similar to breast tumorigenesis. Depletion of CtIP evokes a similar phenotype (unpublished data). To identify the genes that are directly coregulated by the two proteins during this process, we performed microarray analyses on MCF10A cells depleted of BRCA1 or CtIP by adenoviral RNAi and grown in 3D culture for 15 hr. Among over a hundred genes with altered expression profiles, only a dozen were concomitantly upregulated (fold > 2; $p < 0.05$) in both sets of experiments (Table 1), suggesting that they are corepressed by BRCA1 and CtIP. At least five of them, the upregulations of which were confirmed by RT-PCR (Figure S1 in the Supplemental Data available with this article online), are proliferation markers, including *ANG1*, *bFGF*, *HMGA2*, *LIMK1*, and *RFC1* (Caine et al., 2003; Cullmann et al., 1995; Davila et al., 2003; Imura et al., 2004; Tessari et al., 2003). We were particularly intrigued by *ANG1*, a secreted angiogenic factor modulating the tumor microenvironment. ANG1 promotes tubular formation and survival of endothelial cells and enhances blood vessel growth and maturation upon binding to Tie2 receptor tyrosine kinase on the endothelial cell surface (Hayes et al., 1999; Kwak et al., 1999; Suri et al., 1996). Dysfunction of BRCA1 is correlated with accelerated growth and progression of breast tumors (Stoppa-Lyonnet et al., 2000; Xu et al., 1999), often displaying microvascular proliferation (Goffin et al., 2003). Consistently, we observed that *Brca1*-deficient mouse mammary tumors exhibit pronounced growth and extensive enlargement of vasculature (Table 2).

To verify our microarray data showing that a decrease of BRCA1 (−7.9-fold) or CtIP (−3.9-fold) in MCF10A cells evoked a significant increase of ANG1 (+2.7- or +2.4-fold, respectively) (Figures 1A and 1B), we performed RT-PCR on MCF10A cells in 3D culture. Reduced expression of BRCA1 or CtIP paralleled increased ANG1 expression (Figures 1C and 1D), suggesting that a deficiency of either BRCA1 or CtIP upregulates ANG1 expression.

The interaction between BRCA1 and CtIP is required for transcriptional repression of the ANG1 promoter

BRCA1 and CtIP both serve as transcriptional corepressors and interact with each other. To determine a potential transcriptional regulation of ANG1 by BRCA1 and CtIP, we measured the luciferase reporter activity of *ANG1* promoter constructs with different lengths (Figure 2A) after BRCA1 or CtIP was depleted in MCF10A cells by adenoviral RNAi. Only construct C, encoding a 3 kb full-length *ANG1* promoter, showed a significant increase in the activity as BRCA1 level decreased by increasing adenoviral RNAi (Figures 2B and 2C), suggesting that the region −3040 to −1799 is essential for transcriptional repression by BRCA1. Similar results were obtained in both 2D monolayer and 3D cultures, independent of the experimental systems. Likewise, as CtIP was depleted by adenoviral RNAi, construct C showed a comparable increase in the activity (Figure 2D). These results

Table 2. Blood vessel area of $p53^{\Delta5\text{–}6/\Delta5\text{–}6}$ and $Brca1^{\Delta11/\Delta11};p53^{\Delta5\text{–}6/\Delta5\text{–}6}$ mouse mammary tumors

Genotype	Mouse ID	Tumor vol.[a] (ml)	Latency (months)	Blood vessel luminal area[b] (μm^2)
$p53^{\Delta5\text{–}6/\Delta5\text{–}6}$ (n = 14)				
	9108	1.767	16.5	93.0 (±58.6)
	9128	0.666	18.0	84.5 (±55.8)
	9133	0.762	16.5	66.2 (±39.4)
	9207	0.635	15.0	62.4 (±32.1)
	[9268]	0.831	21.2	41.0 (±15.6)
	9270	0.831	16.4	49.8 (±15.8)
	9288	0.606	17.3	59.4 (±28.2)
	9311	0.697	19.2	69.1 (±31.1)
	9323	0.762	16.2	94.0 (±54.8)
	9326	0.762	17.1	90.0 (±40.3)
	9339	1.888	21.4	164.4 (±88.9)
	[9342]	2.145	21.5	141.2 (±95.5)
	[9345]	2.145	20.5	79.5 (±60.1)
	[9349]	0.635	19.0	64.1 (±36.2)
	mean	1.072	18.3	82.8*
	SD	±0.588	±2.2	±33.9
$Brca1^{\Delta11/\Delta11};p53^{\Delta5\text{–}6/\Delta5\text{–}6}$ (n = 17)				
	[741]	1.767	3.9	329.8 (±209.2)
	806	0.831	8.2	161.3 (±81.2)
	[820]	2.424	6.5	313.4 (±226.4)
	[824]	1.337	6.2	310.8 (±75.1)
	847	0.831	6.4	160.3 (±39.9)
	876	0.762	6.4	381.2 (±131.6)
	[905]	0.905	6.9	139.4 (±95.1)
	913	1.437	6.9	157.6 (±76.3)
	942	0.905	7.1	90.3 (±21.7)
	945	1.064	6.5	111.2 (±38.4)
	947	0.905	3.4	206.7 (±90.5)
	960	0.697	5.9	126.0 (±64.5)
	986	0.762	4.9	182.4 (±63.7)
	1043	0.831	4.4	582.3 (±309.1)
	1094	0.697	6.8	102.2 (±41.3)
	1114	0.831	6.9	95.4 (±43.6)
	1133	0.762	6.4	361.0 (±32.6)
	mean	0.996	6.1	224.2*
	SD	±0.460	±1.3	±135.0

Tumor samples used for photographic display (Figure 6) are indicated in brackets. *p = 0.000672.

[a] Tumor volume = $\pi/6\ [(L + W + D)/3]^3$.

[b] Average luminal area of blood vessels (n = 400–600) for each tumor sample (±SD).

imply that the region (−3040/−1799) of *ANG1* promoter is subject to corepression by BRCA1 and CtIP.

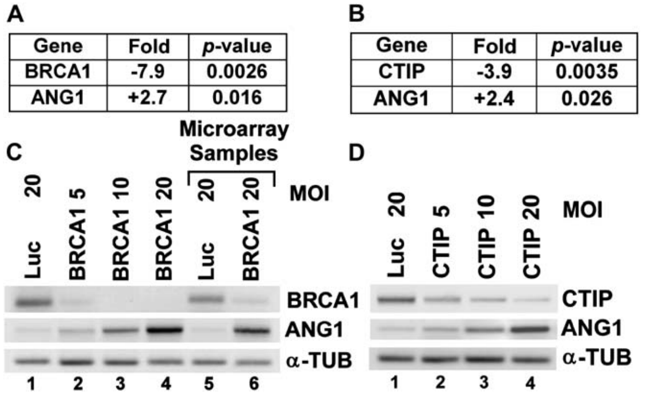

Figure 1. ANG1 is corepressed by BRCA1 and CtIP in MCF10A cells

A: Microarray data of relative expression levels of BRCA1 and ANG1 in MCF10A cells infected with adenoviral BRCA1- versus luciferase-RNAi at 20 MOI for 24 hr and grown in 3D culture for 15 hr.

B: Microarray data of relative expression levels of CtIP and ANG1 in MCF10A cells infected with adenoviral CtIP- versus luciferase-RNAi at 20 MOI for 24 hr and grown in 3D culture for 15 hr.

C: RT-PCR analysis on BRCA1 and ANG1 expressions in MCF10A cells infected with adenoviral luciferase- or BRCA1-RNAi for 24 hr and grown in 3D culture for 15 hr. α-tubulin (α-TUB) serves as a loading control.

D: RT-PCR analysis on CtIP and ANG1 expressions in MCF10A cells infected with adenoviral luciferase- or CtIP-RNAi for 24 hr and grown in 3D culture for 15 hr. α-tubulin serves as a loading control.

To test if the interaction of BRCA1 and CtIP is required for ANG1 repression, we generated RNAi-resistant BRCA1 and CtIP expression plasmids that are either wild-type or point mutants: C61G (RING domain), Q356R (central region), and M1775R (BRCT domain) for BRCA1; and S327A for CtIP. A mutation of BRCA1 at M1775R impairs binding of a group of BRCT domain-interacting proteins including CtIP, whereas a mutation of CtIP at S327A impedes BRCA1 binding (Yu and Chen, 2004; Yu et al., 1998). Treatment of MCF10A cells with an RNAi-resistant BRCA1 (Figure 2E) or CtIP (Figure 2F) plasmid prior to the cognate adenoviral RNAi infection effectively rescued their expressions. As the luciferase activity of construct C was measured under this context (Figure 2G), cells expressing RNAi-resistant wild-type BRCA1 or CtIP endured the repression despite the increasing adenoviral RNAi. In contrast, cells expressing RNAi-resistant BRCA1M1775R or CtIPS327A mutant failed to repress the activity even at the lowest dose (5 MOI) of adenoviral infection, suggesting that the interaction of BRCA1 and CtIP is essential for repressing ANG1 transcription. Interestingly, BRCA1Q356R mutant, but not BRCA1C61G mutant, also failed to repress ANG1 transcription, indicating that the central region of BRCA1 is also involved in this process.

A single ZBRK1 recognition site in *ANG1* promoter mediates BRCA1 and CtIP corepression

BRCA1 interacts at the central region (aa 341–748) with ZBRK1, which mediates BRCA1-dependent transcriptional repression of certain genes by directly binding to a consensus motif (GGGxxxCAGxxxTTT) (Zheng et al., 2000b). If a ZBRK1 recognition site is indeed present in *ANG1* promoter, a chimeric transactivator, a ZBRK1 DNA binding domain fused to a VP16 transactivation domain, would recognize this sequence and upregulate the *ANG1* promoter activity (Zheng et al., 2000b). As shown in Figure 3A, the presence of this chimeric ZBRK1 promoted the luciferase reporter activity of construct C, but not A or B, suggesting that the region −3040 to −1799 contains potential ZBRK1 recognition sites involved in transcriptional repression of ANG1 by ZBRK1. Sequence analyses revealed that this region contains a total of five potential ZBRK1 binding sites. To map a functional ZBRK1 binding site, we generated deletion mutants in the first three ZBRK1 binding sites (C1: Δ−2600/−2200), the last two sites (C2: Δ−2200/−1800), and all the five sites (C3: Δ−2600/−1800) (Figure 3B). Reporter assays showed that C1 and C3, but not C2, were repression defective, and neither BRCA1 (Figure 3C) nor CtIP depletion (Figure 3D) further derepressed the activities. Sequence analysis of the first three potential sites revealed a nearly canonical ZBRK1 consensus motif (−2310/−2296: GAGxxxCAGxxxTTT). We then generated a mutant construct, C-mt-Z, by substituting the five essential nucleotides (GTTxxTTTGxxxTTT) (Figure 3B) and found that this mutant

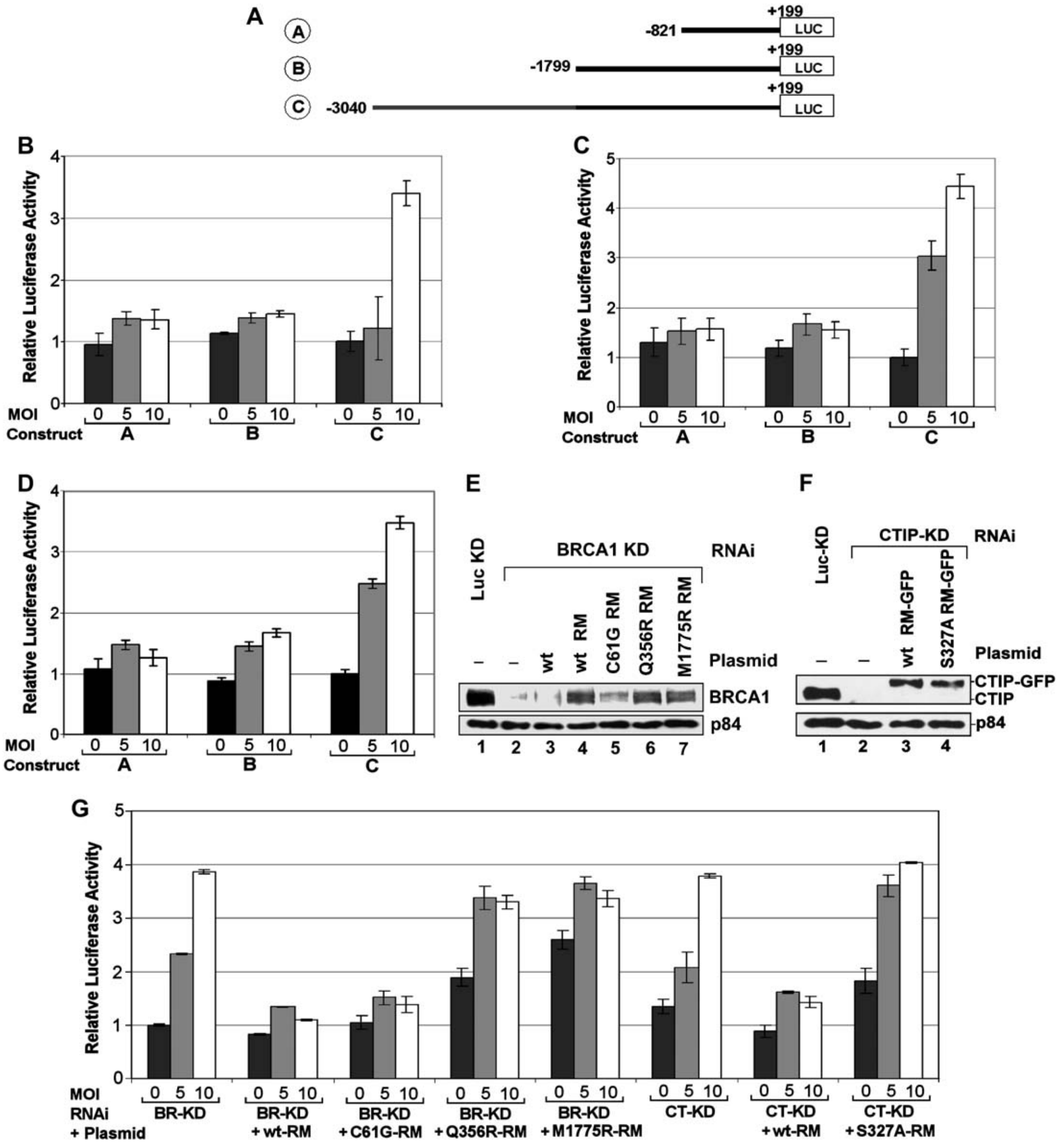

Figure 2. Interaction of BRCA1 and CtIP is required for transcriptional repression of *ANG1* promoter

A: Schematics of *ANG1* reporter constructs A–C in the promoter region. A, −821/+199; B, −1799/+199; and C, −3040/+199 from the start codon.

B: Relative luciferase activity of reporter constructs A–C in MCF10A cells infected with adenoviral BRCA1-RNAi for 24 hr in 2D monolayer culture. Error bar, ±SD.

C: Relative luciferase activity of reporter constructs A–C in MCF10A cells infected with adenoviral BRCA1-RNAi for 24 hr in 3D culture. Error bar, ±SD.

D: Relative luciferase activity of reporter constructs A–C in MCF10A cells infected with adenoviral CtIP-RNAi for 24 hr in 2D monolayer culture. Error bar, ±SD.

E: Western analysis on the expression of BRCA1 (wt, C61G, Q356R, or M1775R) after treatment with an RNAi-resistant (RM) construct prior to adenoviral BRCA1-RNAi infection. p84 serves as a loading control.

F: Western analysis on the expression of GFP-CtIP (wt or S327A) after treatment with an RNAi-resistant (RM) construct prior to adenoviral CtIP-RNAi infection. p84 serves as a loading control.

G: Relative luciferase activity of reporter construct C in MCF10A cells treated with an RNAi-resistant BRCA1 (wt, C61G, Q356R, or M1775R) or CtIP (wt or S327A) prior to the cognate adenoviral RNAi infection (BR, BRCA1; CT, CtIP). Error bar, ±SD.

responded to repression by neither BRCA1 (Figure 3C), CtIP (Figure 3D), nor ZBRK1 (Figure 3A), suggesting that this putative site (−2310/−2296) is a strong candidate for a ZBRK1 binding site.

To test whether ZBRK1 directly binds to this putative site, a 33-mer radiolabeled oligonucleotide probe (−2319/−2287) harboring the ZBRK1 recognition site (−2310/−2296) of *ANG1* promoter (wt-Z) was used to perform an electromobility shift assay (EMSA) using either GST-fused ZBRK1 eight-Zn finger domain (Zheng et al., 2000b) or nuclear extract. We included a nonlabeled wt (wt-Z) or point mutant ZBRK1 (mt-Z) binding sequence of *ANG1* promoter and AP12, a canonical consensus ZBRK1 binding sequence (Zheng et al., 2000b), for competition experiments. As expected, a nonlabeled wild-type *ANG1* or AP12 competitor, but not mutant *ANG1*, competed with a labeled wild-type probe for binding ZBRK1, suggesting that ZBRK1 directly binds to this site (−2310/−2296) (Figure 3E). To further demonstrate that this ZBRK1 recognition site is functional in vivo, we generated a heterologous reporter construct with a 800 bp fragment (−2600/−1800) containing a wild-type (3P-26-wt-Z) or mutant (3P-26-wt-Z) ZBRK1 binding site (−2310/−2296) (Figure 3F). Reporter assay showed that the activity increased as ZBRK1 level decreased by increasing

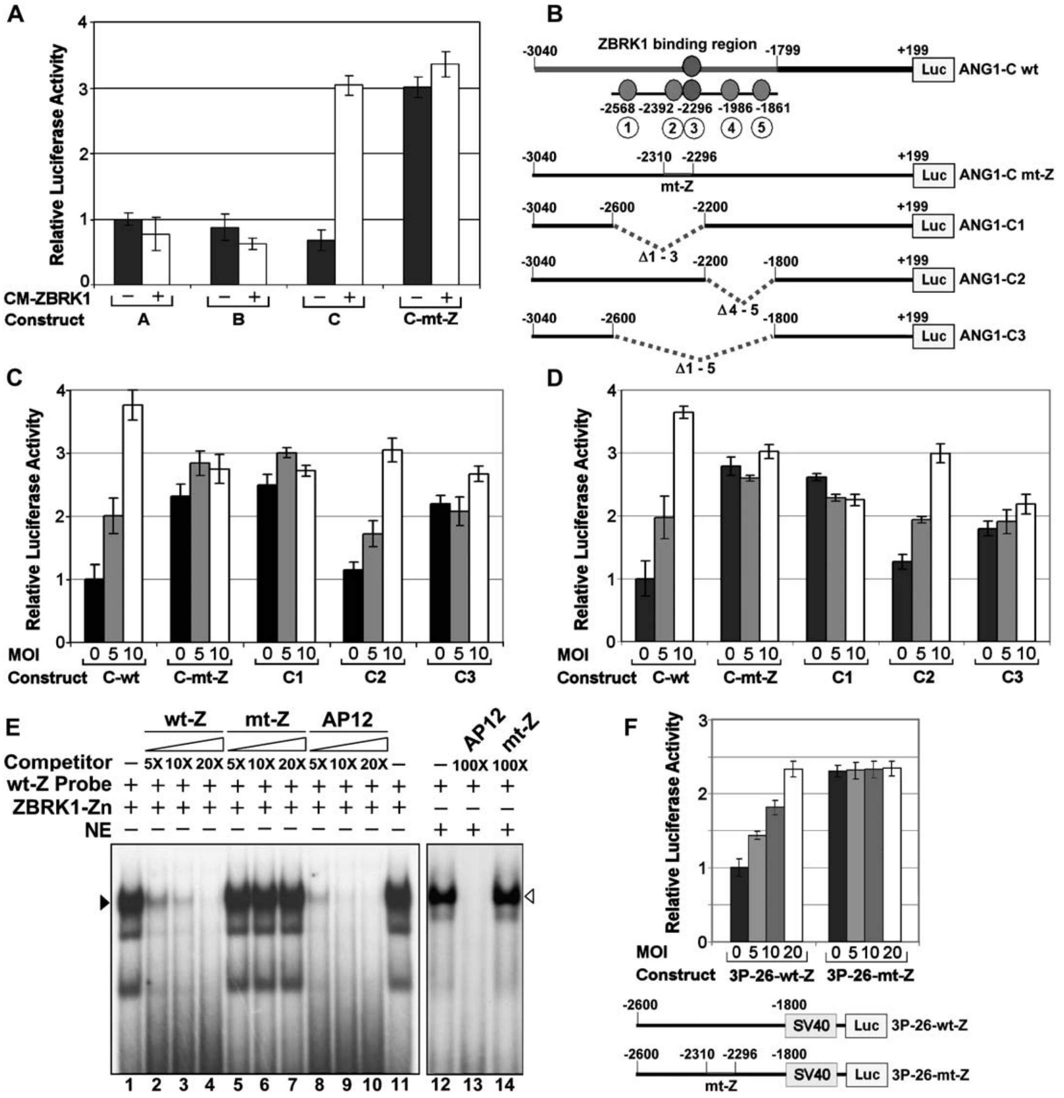

Figure 3. BRCA1, CtIP, and ZBRK1 corepress ANG1 expression via a single ZBRK1 recognition element in the promoter

A: Relative luciferase activity of *ANG1* reporter constructs A–C and C-mt-Z, a point mutant in a putative ZBRK1 binding site (−2310/−2296), in MCF10A cells expressing a chimeric (CM) ZBRK1 where the KRAB repression domain is replaced with the VP16 activation domain. Error bar, ±SD.

B: Schematics of *ANG1* reporter constructs derived from construct C. C-wt, wild-type (−3040/+199) containing five potential ZBRK1 binding sites; C-mt-Z, a point mutant in a putative ZBRK1 binding site (−2310/−2296); C1, a deletion of the first three binding sites (Δ−2600/−2200); C2, a deletion of the last two binding sites (Δ−1200/−1800); and C3, a deletion of all the five binding sites (Δ−2600/−1800).

C: Relative luciferase activity of reporter construct C derivatives in MCF10A cells after infection with adenoviral BRCA1-RNAi for 24 hr. Error bar, ±SD.

D: Relative luciferase activity of reporter construct C derivatives in MCF10A cells after infection with adenoviral CtIP-RNAi for 24 hr. Error bar, ±SD.

E: EMSA on a competition between a radiolabeled wild-type ZBRK1 site (−2310/−2296) in *ANG1* promoter (wt-Z, 33 mer) and a nonlabeled competitor for binding GST-ZBRK1-Zn protein (the eight-zinc finger domain) or ZBRK1 in nuclear extract (NE). The competitors used are wild-type (wt-Z) or a point mutant (mt-Z) of a ZBRK1 site (−2310/−2296) in *ANG1* promoter (33 mer) and a canonical ZBRK1 binding sequence (AP12, 29 mer).

F: (Top) Relative luciferase activity of a regulatory region (−2600/−1800) in *ANG1* promoter with a wild-type (3P-26-wt-Z) or point mutant (3P-26-wt-Z) of a putative ZBRK1 binding site (−2310/−2296) in MCF10A cells after infection with adenoviral ZBRK1-RNAi for 24 hr. Error bar, ±SD. (Bottom) Schematics of *ANG1* reporter constructs used. 3P-26-wt-Z, a fragment composed of a regulatory region; and 3P-26-mt-Z, a fragment of a regulatory region with point mutations in a ZBRK1 binding site.

adenoviral ZBRK1 RNAi (see below Figure 4A), whereas a mutant ZBRK1 site was repression defective (Figure 3F), further confirming that this site is an authentic ZBRK1 recognition site.

ZBRK1, BRCA1, and CtIP form a repressor complex on *ANG1* promoter

Since BRCA1/CtIP corepresses *ANG1* promoter via a ZBRK1 recognition site, it is expected that depletion of ZBRK1 would derepress *ANG1* expression, similar to the effect of BRCA1 and CtIP depletion (Figure 1A). To test this possibility, we depleted ZBRK1 by adenoviral mediated RNAi in MCF10A cells in 3D culture and assessed the ANG1 expression level using RT-PCR. Reduced ZBRK1 expression paralleled increased ANG1 expression (Figure 4A), suggesting that a deficiency of ZBRK1 upregulates *ANG1* repression. These results altogether implicate that ZBRK1, BRCA1, and CtIP coordinately repress

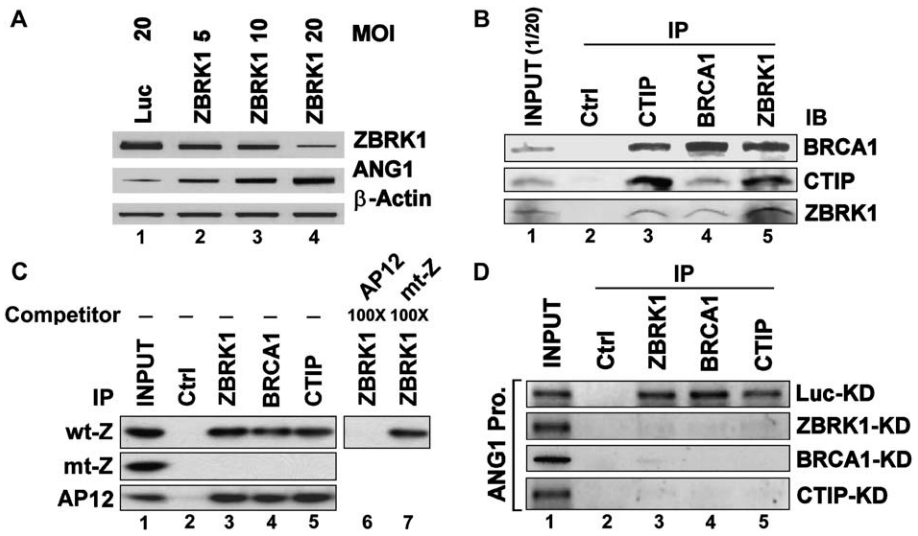

Figure 4. ZBRK1, BRCA1, and CtIP form a repressor complex on *ANG1* promoter

A: RT-PCR analysis on ZBRK1 and ANG1 expressions in MCF10A cells infected with adenoviral luciferase- or ZBRK1-RNAi for 24 hr and grown in 3D culture for 15 hr. β-actin serves as a loading control.

B: Reciprocal coimmunoprecipitation of CtIP, BRCA1, and ZBRK1 from nuclear extract.

C: DNA immunoprecipitation by antibodies against ZBRK1, BRCA1, and CtIP from nuclear extract mixed with an oligonucleotide probe encompassing a ZBRK1 binding sequence (wt-Z, mt-Z, or AP12).

D: ChIP analysis on a 300 bp fragment around a ZBRK1 binding site in *ANG1* promoter (−2400/−2100) to detect the association of BRCA1, CtIP, and ZBRK1 in MCF10A cells infected with adenoviral luciferase-, BRCA1-, CtIP-, or ZBRK1-RNAi at 20 MOI for 24 hr.

ANG1 expression. Since BRCA1 binds CtIP via its BRCT domain (Li et al., 1999) and ZBRK1 via its central domain (Zheng et al., 2000b), it is likely that these three proteins form a repressor complex on the ZBRK1 recognition site. To test this possibility, these three proteins were reciprocally coimmunoprecipitated from nuclear extract (Figure 4B), suggesting that they form a complex. Next, we mixed a radiolabeled oligonucleotide probe containing a wild-type (wt-Z or AP12) or mutant (mt-Z) ZBRK1 binding sequence with nuclear extract for immunoprecipitation. Antibodies against ZBRK1, BRCA1, and CtIP brought down a wild-type (wt-Z or AP12), but not mutant (mt-Z), oligonucleotide specifically (Figure 4C). Finally, to demonstrate that this complex is associated with *ANG1* promoter in vivo, we performed a chromatin immunoprecipitation (ChIP) assay on a 300 bp fragment around the ZBRK1 site (−2400/−2100). As shown in Figure 4D, ZBRK1, BRCA1, and CtIP colocalized on *ANG1* promoter, while an individual depletion of either protein by RNAi completely abolished the association of all the three proteins with the promoter, suggesting that the three participants are all essential for the complex formation. Taken together, these data substantiate a notion that BRCA1, CtIP, and ZBRK1 coordinately form a repressor complex tethered at the ZBRK1 recognition site in *ANG1* promoter.

Expression of ANG1 from MECs is essential for the stability of capillary-like network structures formed by neighboring endothelial cells in 3D matrix

To assess a biological consequence of derepressed ANG1 expression, we cocultured MCF10A cells with human umbilical endothelial cells (HUVECs) in 3D matrix. HUVECs alone formed a thin layer of capillary-like network structure in a day but soon came to disintegrate and died in a week under this experimental condition (Figure 5Ba). When HUVECs were cocultured with luciferase-RNAi/GFP-treated MCF10A cells, they formed a well-defined thin layer of capillary-like structure in a day; however, the endothelial cells, indicated as nonfluorescent cells, started to die in 3 days, and the capillary-like structure disintegrated in a week (Figure 5Bb). When HUVECs unlabeled (Figure 5Be) or labeled with histone H2B/GFP (Figure 5Bf) were cocultured with MCF10A/ANG1 cells that stably express ANG1 by retroviral infection (Figure 5A), they formed a thick layer of capillary-like structure, which sustained over a week. When HUVECs were cocultured with MCF10A cells infected with BRCA1-RNAi/GFP (Figure 5Bc) or CtIP-RNAi/GFP (Figure 5Bd) adenovirus, they formed a thick layer of capillary-like structure, which maintained for a week in a manner similar to those cocultured with MCF10A/ANG1 cells. To validate the essential role of ANG1 in the survival of cocultured endothelial cells, we treated MCF10A cells with ANG1 siRNA, which was shown by Western analysis to completely deplete ANG1 in MCF10A/ANG1 cells after 36 hr (Figure 5C). HUVECs cocultured with ANG1 siRNA-treated MCF10A/ANG1 cells formed a thin layer of capillary-like structure in a day but soon came to disintegrate and died after a week (Figure 5Dh) in a manner similar to those cocultured with Luc-RNAi/GFP-infected MCF10A cells (Figures 5Da and 5Db). Likewise, when HUVECs were cocultured with MCF10A cells treated with ANG1 siRNA prior to BRCA1-RNAi/GFP (Figure 5Dd) or CtIP-RNAi/GFP (Figure 5Df) adenoviral infection, they formed a thin layer of capillary-like structure in a day, but the endothelial cells, indicated as nonfluorescent cells, started to disintegrate after 3 days and died in a week, leaving aggregates of fluorescent MECs. Based on these observations, upregulated expression of ANG1 from MECs, either by the overexpression construct or by depletion of BRCA1 or CtIP, is essential for the stability of capillary-like structures formed by the cocultured endothelial cells in 3D matrix.

Brca1-deficient mouse mammary tumors exhibit an accelerated growth and harbor enlarged blood vessels along with upregulated Ang1 expression

To test if these in vitro observations gain support from animal studies, we examined mammary tumor samples from *Brca1*-deficient mice. *BRCA1*-associated tumorigenesis is often linked to a loss of *p53* (Xu et al., 1999). To recapitulate the *BRCA1*-related tumor pathogenesis, we used a mouse model inactivated in both *Brca1* and *p53* genes ($Brca1^{\Delta 11/\Delta 11};p53^{\Delta 5-6/\Delta 5-6}$) (n = 17) in comparison to mice inactivated only in *p53* gene ($p53^{\Delta 5-6/\Delta 5-6}$) (n = 14) as a control (Lin et al., 2004; Xu et al., 1999). *Brca1*-deficient tumors exhibited a substantially shorter latency than control tumors (6.1 ± 1.3 versus 18.3 ± 2.2 months) to reach a comparable size (0.996 ± 0.460 versus 1.072 ± 0.588 ml, respectively) (Table 2). In general, *Brca1*-deficient tumors

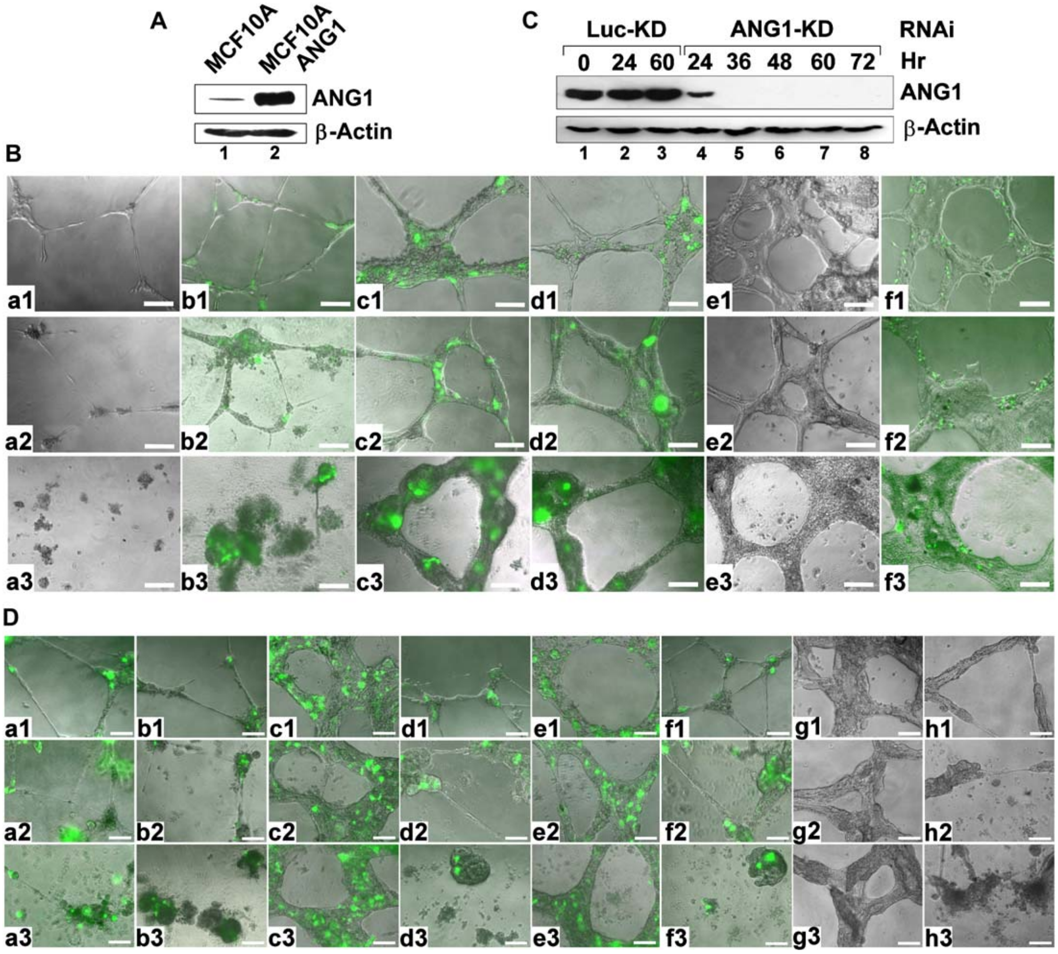

Figure 5. Expression of ANG1 from MECs is essential for the survival of HUVECs and stability of the capillary-like structure in 3D matrix

A: Western analysis of ANG1 expression in MCF10A/ANG1 cells in comparison to the parental MCF10A cells.

B: Survival of HUVECs and stability of the capillary-like structure in 3D matrix. Images were captured with Phase I/FITC reflector at 100× magnification. **Ba:** HUVECs only. **Bb:** HUVECs cocultured with adenoviral luciferase-RNAi/GFP-infected MCF10A cells. **Bc:** HUVECs cocultured with adenoviral BRCA1-RNAi/GFP-infected MCF10A cells. **Bd:** HUVECs cocultured with adenoviral CtIP-RNAi/GFP-infected MCF10A cells. **Be:** HUVECs cocultured with MCF10A/ANG1 cells. **Bf:** HUVECs marked with histone H2B/GFP and cocultured with MCF10A/ANG1 cells. (1) 24 hr, (2) 3 days, and (3) 7 days of growth in 3D culture. Adenoviral RNAi infection was performed at 20 MOI for 24 hr. Scale bar, 50 μm.

C: Western analysis on ANG1 expression in MCF10A/ANG1 cells treated with luciferase or ANG1 siRNA for a different period of time.

D: Pretreatment of MCF10A cells with ANG1 siRNA destabilizes the capillary-like structure formed by HUVECs in 3D matrix. Images were captured with Phase I/FITC reflector at 100× magnification. **Da and Db:** HUVECs cocultured with MCF10A cells pretreated with luciferase (**Da**) or ANG1 (**Db**) siRNA prior to adenoviral luciferase-RNAi/GFP infection at 20 MOI for 24 hr. **Dc and Dd:** MCF10A cells pretreated with luciferase (**Dc**) or ANG1 (**Dd**) siRNA prior to adenoviral BRCA1-RNAi/GFP infection at 20 MOI for 24 hr. **De and Df:** MCF10A cells pretreated with luciferase (**De**) or ANG1 (**Df**) siRNA prior to adenoviral CtIP-RNAi/GFP infection at 20 MOI for 24 hr. **Dg and Dh:** HUVECs cocultured with MCF10A/ANG1 cells pretreated with luciferase (**Dg**) or ANG1 (**Dh**) siRNA. (1) 24 hr, (2) 3 days, and (3) 7 days of growth in 3D culture. Adenoviral RNAi infection was performed at 20 MOI for 24 hr. Scale bar, 50 μm.

displayed an ensanguined appearance, noticeably distinct from control tumors with the same size (Figure 6A). To examine the blood vessel status of these tumor specimens, they were stained against CD31, an endothelial cell marker (Machein et al., 2004). Apparently, *Brca1*-deficient tumors contained larger blood vessels compared to control tumors (Figures 6B and 6C). The blood vessel luminal area of *Brca1*-deficient tumor was almost three times the size of that of the control tumor (224.2 ± 135.0 versus 82.8 ± 33.9 μm^2; $p < 0.001$) (Table 2), while microvascular density (mm^2) did not significantly differ between the two sets of tumors ($p = 0.22$; data not shown), consistent with a finding that ANG1 causes vessel enlargement without angiogenic sprouting during development (Thurston et al., 2005). Interestingly, analogous regulatory elements, including a ZBRK1 recognition site, were found in the mouse *Ang1* promoter region (Figure 6D), suggesting that mouse Ang1 expression may be subjected to a similar mode of regulation as human. Consistently, Ang1 expression was mostly upregulated in *Brca1*-deficient tumors, but not in control tumors (Figure 6E). Taken together, these results support a notion that inactivation of *BRCA1* in MECs upregulates ANG1 expression to support formation of large blood vessels.

Discussion

BRCA1 plays an essential role in DNA damage response and cell cycle checkpoint control, which are intimately linked to a restraint of cancer initiation. Additional functions of BRCA1 remain

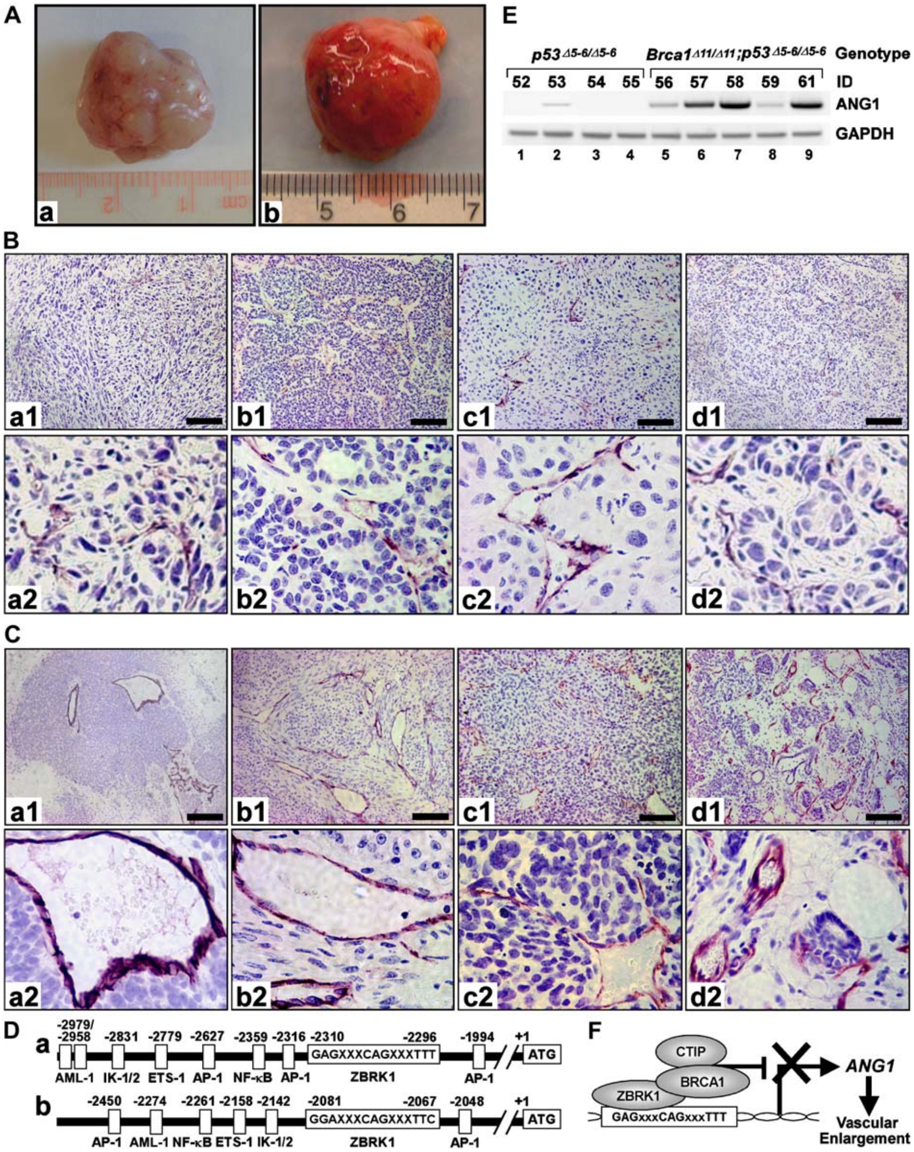

Figure 6. *Brca1*-deficient mouse mammary tumors exhibit enlarged blood vessels and overexpressed ANG1

A: Whole mammary tumors (~1.8 cm in diameter) excised from *p53*$^{\Delta5–6/\Delta5–6}$ (**Aa**) and *Brca1*$^{\Delta11/\Delta11}$;*p53*$^{\Delta5–6/\Delta5–6}$ (**Ab**) mice.

B: Mammary tumor sections from *p53*$^{\Delta5–6/\Delta5–6}$ mice stained for CD31 (brown) and counterstained with hematoxylin. Mouse ID: 9268 (**Ba**), 9342 (**Bb**), 9345 (**Bc**), and 9349 (**Bd**). Images were captured at 200× (1) and at 1000× (2) magnifications. Scale bar, 50 μm.

C: Mammary tumor sections from *Brca1*$^{\Delta11/\Delta11}$;*p53*$^{\Delta5–6/\Delta5–6}$ mice stained for CD31 (brown) and counterstained with hematoxylin. Mouse ID: 741 (**Ca**), 820 (**Cb**), 824 (**Cc**), and 905 (**Cd**). Images were captured at 200× (1) and at 1000× (2) magnifications. Scale bar, 50 μm.

D: *ANG1* promoter region in human (**Da**) and mouse (**Db**) around a ZBRK1 binding site with conserved transcriptional regulatory elements. AML-1, acute myeloid leukemia protein-1; AP-1, activator protein-1; ETS-1, v-ets erythroblastosis virus E26 oncogene homolog 1; IK-1/2, Ikaros 1/2; NF-κB, nuclear factor kappa B.

E: Ang1 expression in *p53*$^{\Delta5–6/\Delta5–6}$ and *Brca1*$^{\Delta11/\Delta11}$;*p53*$^{\Delta5–6/\Delta5–6}$ mouse mammary tumors detected by RT-PCR. GAPDH serves as an internal control.

F: A schematic for ANG1 transcriptional repression by BRCA1, CtIP, and ZBRK1 via a ZBRK1 recognition site in the promoter.

to be further characterized. In this communication, we reveal that BRCA1, in coordination with CtIP and ZBRK1, exerts a transcriptional repression on ANG1 that pertains to cancer progression. To mimic in vivo conditions, we depleted BRCA1 and CtIP in normal MECs cultured in extracellular matrix. Microarray analyses identified a dozen genes corepressed by BRCA1 and CtIP. We focused on *ANG1* since it may participate in cancer progression through angiogenesis. Our results demonstrated that BRCA1 and CtIP, along with ZBRK1, form a repressor complex on *ANG1* promoter via a ZBRK1 recognition element (Figure 6F) and that *Brca1*-deficient mouse mammary tumors exhibit prominent vascularization and accelerated growth along with Ang1 upregulation. This suggests that derepressed ANG1 expression in MECs in the absence of BRCA1 is a pathogenic drive for neoplastic growth.

Depletion of BRCA1 impairs acinar differentiation but promotes proliferation of MECs into a tumor-like aggregate in 3D culture (Furuta et al., 2005). Strikingly, our preliminary results showed that depletion of CtIP as well as ZBRK1 leads to a phenotype identical to BRCA1 depletion, suggesting that they share at least one common regulation pathway. ZBRK1, a sequence-specific transcriptional repressor that binds to the canonical GGGxxxCAGxxxTTT motif, interacts with the central region of BRCA1 (aa 341–748) and mediates the transcriptional repression activity of BRCA1 (Zheng et al., 2000b). Interestingly, there are five potential ZBRK1 sites in *ANG1* promoter due to the degeneracy of the consensus motif, but only one site (nt −2310/−2296) has the in *cis* transcriptional repression function, since point mutations at this site abolished the capacity (Figure 3). Through this recognition site, ZBRK1, BRCA1, and CtIP form a repressor complex on *ANG1* promoter. This conclusion was supported by the following observations. First, a defect in BRCA1, CtIP, and ZBRK1 complex formation on *ANG1* promoter, caused by lacking one of the participants or their interactions, impairs ANG1 transcriptional repression. Second, BRCA1, CtIP, and ZBRK1 can be coimmunoprecipitated with an oligonucleotide containing the wild-type ZBRK1 recognition sequence. Third, by ChIP analysis, BRCA1, CtIP, and ZBRK1 colocalized at *ANG1* promoter. It is noted that depletion of one of these three components leads to disassembly of the entire repressor complex including ZBRK1, suggesting that the stability of ZBRK1 binding to the recognition site depends on the integrity of the complex. This is inconsistent with the result from an in vitro binding assay showing that ZBRK1 alone binds to its consensus sequence. How to reconcile this discrepancy remains unclear. Nevertheless, BRCA1 was shown to facilitate ZBRK1 binding to the recognition site in vivo (Tan et al., 2004), and CtIP is also likely to contribute in a similar manner, although the precise architecture of this complex binding to ZBRK1 site remains to be elucidated.

Apparently, the regulation of *ANG1* promoter would be more complicated than that by a repressor complex alone. Since a point mutation in the ZBRK1 binding site (−2310/−2296) as well as a deletion in the surrounding region (Δ−2600/−1800) upregulated ANG1 transcription (Figure 3), the region −2310 to −2296 must be involved in repression, while the region outside (−3040/−2600) must be involved in activation once the repression is removed. It is probable that derepression of ANG1 in the region −2310/−2296 evokes a subsequent activation of the neighboring region by altering the local chromatin structure to allow the accessibility to certain transactivators. In fact, the region around the ZBRK1 binding site in *ANG1* promoter encompasses various conserved transcriptional regulatory elements, such as AML1 (CBF-α/CBFA2) (Figure 6D), which is responsible for upregulation of ANG1 expression during embryogenesis (Brown et al., 2004; Takakura et al., 2000). Clearly, derepression is the first step for full activation of the promoter. The mechanisms of how the repressor complex is removed from the ZBRK1 site and how these two steps are coordinated in regulating *ANG1* promoter warrant further investigation.

Angiogenesis is a critical process for tumor progression. ANG1 promotes tubular formation and survival of endothelial cells (Hayes et al., 1999; Kwak et al., 1999) and enhances blood vessel growth and maturation (Suri et al., 1996). Consistently, we observed that ANG1 expressed from MECs exerts a paracrine action on neighboring endothelial cells for their survival and stability of capillary-like network structures. *Brca1*$^{\Delta 11/\Delta 11}$;*p53*$^{\Delta 5-6/\Delta 5-6}$ mouse mammary tumors, characterized by their accelerated growth and ensanguined appearance, harbor prominently enlarged blood vessels compared to *p53*$^{\Delta 5-6/\Delta 5-6}$ mouse mammary tumors. Such a phenotype of *Brca1*-deficient mammary tumors may be attributed to derepressed ANG1 expression from MECs, stabilizing the adjacent blood vessels and promoting their growth to provide conduits for supplying nutrition as well as removing waste, consistent with the observation that ANG1 causes vessel enlargement without angiogenic sprouting during development (Thurston et al., 2005). Furthermore, gliomas overexpressing ANG1 exhibit accelerated tumor growth and extensive vasculature (Machein et al., 2004), a phenotype similar to *Brca1*$^{\Delta 11/\Delta 11}$;*p53*$^{\Delta 5-6/\Delta 5-6}$ mouse mammary tumors. Although it is yet to be examined whether *BRCA1*-associated human breast tumors harbor enlarged blood vessels as observed in mice, these tumors metastasize to a distant site through the bloodstream instead of lymphatic routes (Foulkes et al., 2003), suggesting that they develop blood vessels much earlier than non-*BRCA1*-associated tumors. Our observation in mice provides a likely explanation of this clinical manifestation.

In addition to *ANG1*, one of the identified genes *bFGF* is also involved in angiogenesis (Imura et al., 2004), while several other genes, *HMGA2*, *LIMK1*, and *RFC1*, are involved in proliferation (Cullmann et al., 1995; Davila et al., 2003; Tessari et al., 2003). As the net effect, an impaired transcriptional repression activity of BRCA1 and CtIP will promote angiogenic and proliferative potentials of cells. Currently, we are examining if the remaining genes are regulated under a similar mechanism as *ANG1*, aiming to further understand the cellular events involved in the progression of *BRCA1*- and *CtIP*-associated tumors.

A neoplastic potential due to a dysfunction of BRCA1 tumor suppressor has been largely ascribed to the genomic instability resulting from defects in DNA damage-responsive pathways. However, the present study shows that BRCA1 deficiency modulates the tissue microenvironment by derepression of ANG1 (or bFGF) that promotes the growth of adjacent vasculature in a paracrine fashion to nourish a neoplasm. Moreover, an aberrant activity of a BRCA1-interacting partner, CtIP tumor suppressor, also deregulates ANG1 expression, which may likewise pertain to the etiology of tumor growth in *Ctip* heterozygous mice (Chen et al., 2005). Apparently, these two tumor suppressors have much broader activities than other tumor susceptibility genes, such as MSH2 and ATM, which exclusively play roles in guarding genomic stability. This study concludes that BRCA1 and CtIP possess an additional role in tumor suppression, via a ZBRK1 element, by regulating the intercellular signaling within the tissue microenvironment besides maintaining the genomic stability within the cell. This view will extend their tumor suppression functions to the surroundings that influence the fate of neighboring cells and fortify the pathogenic relevance of their defect to neoplastic growth.

Experimental procedures

Cell cultures

Human mammary epithelial MCF10A cells and umbilical endothelial cells (HUVECs) were cultured as described (Debnath et al., 2003; Shekhar et al., 2000), respectively.

Adenoviral RNAi construction

The adenovirus-based RNAi vector was generated by cloning an expression cassette of U6 promoter-BRCA1, -CtIP, or -ZBRK1 short hairpin RNAi (0.4 kb) into pAdTrack plasmid upstream of a CMV-GFP cassette (1.6 kb) (He et al., 1998; Sui et al., 2002). The target sequences are as follows: BRCA1, 5′-GGCTACAGAAACCGTGCCAAA-3′; CtIP, 5′-GGGAGCAGACCTTTCTCAGTA-3′; and ZBRK1, 5′-AAACCATGTCATGAACATGAT-3′. Adnoviruses were produced as described (Furuta et al., 2005). MCF10A cells seeded at 5 × 10^5 cells/60 mm plate were infected with adenovirus at a designated MOI for 24 hr.

RNAi-resistant BRCA1 and CtIP plasmids

The RNAi-targeted nucleotide sequence in a full-length BRCA1 cDNA, the expression of which was driven by a CMV promoter in CHpL vector (Li et al., 1999), was partially substituted without affecting the amino acid residues (5′-GGCTACCGGAATAGGGCCAAA-3′), and a cancer-linked point mutation of BRCA1 at C61G, Q356R, or M1775R was introduced into the wild-type RNAi-resistant construct using a site-directed mutagenesis kit (Stratagene). Similarly, the RNAi-targeted nucleotide sequence in GFP-CtIP construct, containing a full-length CtIP cDNA N-terminally fused to GFP (Li et al., 2001), was partially substituted as follows: 5′-GGGAGCTGACTTGTCTCAGTA-3′, and a point mutation of CtIP at S327A was introduced into the wild-type RNAi-resistant construct. Correct substitutions were confirmed by sequencing. Respective primer sequences used are shown in Table S1. MCF10A cells seeded at 5 × 10^5 cells/60 mm plate were transfected with 3 μg of RNAi-resistant construct using Fugene6 (Roche) prior to adenoviral RNAi infection.

Microarray and RT-PCR

MCF10A cells seeded at 5 × 10^5 cells/60 mm plate were infected with adenoviral luciferase-, BRCA1-, CtIP-, or ZBRK1-RNAi in duplicate at 20 MOI for

24 hr. Infected cells were reseeded at 5 × 10^5 cells in a 60 mm plate precoated with Growth Factor Reduced Matrigel (BD Biosciences) and covered with the growth medium containing 2% Matrigel at 37°C for 15 hr. RNA was extracted from these cells with Trizol (Invitrogen), clarified by RNeasy spin column (Quiagen), and quality assessed. cDNA synthesized from the harvested RNA using SuperScript Double-Stranded cDNA Synthesis Kit (Invitrogen) served as a template for PCR amplification with respective primers (Table S1), and a portion of it was biotin-labeled using GeneChip IVT Labeling Kit (Affymetrix), hybridized onto Affymetrix HG U133 PLUS 2.0 array (54,676 genes), and stained with streptavidin-phycoerythrin. The hybridized array was analyzed using GeneChip Scanner 3000 and GCOS 1.2 software (Affymetrix) for multiplex pairwise comparison at the UCI Microarray Core service. The statistical significance was evaluated by ANOVA single factor analysis using MS Excel XP, and the fold difference > 2 as well as p value < 0.05 was considered significant. Microarray data are available at Gene Expression Omnibus (GEO; http://www.ncbi.nlm.nih.gov/geo/) with the following accession numbers: BRCA1-KD (GSM106933, GSM106968) versus Luc-KD (GSM106971, GSM106972); and CtIP-KD (GSM106974, GSM106975) versus Luc-KD (GSM106976, GSM106977).

Luciferase reporter assay

ANG1 promoter constructs A (−821/+199), B (−1799/+199), and C (−3040/+199), which regulate luciferase expression in pGL2 vector, were from Peter Oettgen (Harvard Institutes of Medicine, MA) (Brown et al., 2004). Construct C was subjected to site-directed mutagenesis (Stratagene) for deletion mutations of ZBRK1 binding sites: C1 (Δ−2600/−2200), C2 (Δ−1200/−1800), and C3 (Δ−2600/−1800); point mutations of a putative ZBRK1 site (−2310/−2296): C-mt-Z; and for generating a fragment containing ZBRK1 binding sites (−2600/−1800): 3P-26-(wt/mt)-Z with respective primers (Table S1). Correct changes were confirmed by sequencing and restriction digestion.

MCF10A cells seeded at 5 × 10^5 cells/60 mm plate were transfected with 3 μg of luciferase reporter and 0.5 μg of β-galactosidase plasmids using Fugene6 prior to adenoviral RNAi infection. Luciferase and β-galactosidase reporter activities were measured using a reporter assay kit (Promega).

EMSA

EMSA was performed as described (Zheng et al., 2000b). A γ-^{32}P-ATP-labeled oligonucleotide probe (6000 cpm) harboring a ZBRK1 site (−2310/−2296) in *ANG1* promoter (wt-Z, −2319/−2287) was incubated with 50 ng of GST-ZBRK1-Zn protein purified from *E. coli* or 8 μg of MCF10A nuclear extract of in 40 μl of DNA binding buffer containing 1 μg of poly(dI-dC) at room temperature. For competition experiment, molar excess of an unlabeled wild-type or mutant oligonucleotide was included. The sense oligonucleotides used are from wild-type ZBRK1 site in *ANG1* promoter (wt-Z): 5′-ACACACGTG*GAG*GAA*CAG*ATT*TTT*AACAGTCTC-3′; a point mutant of the ZBRK1 site in *ANG1* promoter (mt-Z): 5′-ACACACGTGGTTGATTTGATTTTTAACAGTCTC-3′; and a canonical ZBRK1 binding sequence (AP12) (Zheng et al., 2000b): 5′-GATCCAC*GGG*ACG*CAG*GTG*TTT*TGTGCCG-3′ (ZBRK1 recognition motifs are shown in italics). The reaction was resolved on 5% native polyacrylamide gel at 4°C and autoradiographed.

DNA immunoprecipitation

DNA immunoprecipitation was performed as described (Zheng et al., 2000b). A radiolabeled oligonucleotide of wt-Z, mt-Z, or AP12 was incubated with 50 μg of nuclear extract in 200 μl of DNA binding buffer containing 1 μg of poly(dI-dC) at room temperature for 30 min. The protein-oligonucleotide complex was precipitated by protein G-Sepharose beads loaded with a respective antibody and resolved on 5% polyacrylamide gel followed by autoradiography.

Immunoprecipitation

One microgram of antibody against HA (Ctrl), CtIP, BRCA1, or ZBRK1 was added to 200 μg of preclarified MCF10A nuclear extract and incubated at 4°C overnight. Antibody-protein complex was precipitated by protein G-Sepharose beads and washed with TEN buffer (10 mM Tris-HCl [pH 8.0], 0.25 mM EDTA, 50 mM NaCl). Immunoprecipitates were resolved on 8% SDS-PAGE and detected by Western analysis.

ChIP

ChIP assay was performed as described (Saccani et al., 2001) with a minor modification. Chromatins from 1% formaldehyde-treated MCF10A cells were sonicated to ∼500 bp fragments and immunoprecipitated with antibodies against HA, ZBRK1, BRCA1, and CtIP at 4°C overnight. Chromatin-antibody complexes were washed with buffer 1 (0.1% SDS, 0.5% Triton X-100, 2 mM EDTA, 20 mM Tris-HCl [pH 8.0], 150 mM NaCl), buffer 2 (0.1% SDS, 2 mM EDTA, 20 mM Tris-HCl [pH 8.0], 500 mM NaCl) then TE buffer (10 mM Tris-HCl [pH 8.0], 1 mM EDTA). After reversal of cross-linking, immunoprecipitated chromatin was subjected to PCR reaction for a 300 bp fragment (−2400/−2100) of *ANG1* promoter around a ZBRK1 binding site with respective primers (Table S1).

ANG1 retrovirus and siRNA

A full-length ANG1 cDNA, KIAA0003 clone (GenBank no. D13628) was from Takahiro Nagase (Kazusa DNA Research Institute, Chiba, Japan) (Nomura et al., 1994). A 1.7 kb coding sequence fragment was obtained by PCR reaction with respective primers (Table S1) and cloned into pQCXIH vector (BD Biosciences). GP$_2$-293 packaging cells were transfected with pQCXIH/ANG1 and pVSVG plasmids using Lipofectin, and retrovirus was harvested in the conditioned medium. MCF10A cells were infected with retrovirus using 8 μg/ml polybrene, and the stable clones (MCF10A/ANG1) were selected with 70 μg/ml Hygromycin B (Roche). Overexpression of ANG1 was confirmed by Western analysis using a rabbit anti-ANG1 antibody (1:500, Alpha Diagnostic). ANG1 siRNA was synthesized against the target sequence: 5′-AAGGCTTGGTTACTCGTCAAA-3′ (Qiagen). MCF10A cells seeded at 5 × 10^5 cells/60 mm plate were transfected with 400 pmol of ANG1 or luciferase siRNA for 24 hr using Oligofectamine (Invitrogen) prior to adenoviral infection.

3D coculture

MCF10A cells (5 × 10^4) and HUVECs (5 × 10^4) were seeded together into each well of a 8-well chamber slide coated with Matrigel and covered with SFM supplemented with EGF and bFGF (Shekhar et al., 2000). Fluorescence imaging was performed with Phase I/FITC filters on a Zeiss Axiovert 200M equipped with Hamamatsu Photonics K.K. Deep Cooled Digital Camera using Axiovision 4.4 software.

Mice, histology, and immunohistochemistry

Animal experiments were performed under federal guidelines and approved by the Institutional Animal Care and Use Committee at UCI. Mice with the *p53* gene floxed at exons 5–6 (*p53fp/fp*) were generated as described (Lin et al., 2004). Mice with the *Brca1* gene floxed at exon 11 (*Brca1f11/f11*) were from Chu-Xia Deng (NIH) (Xu et al., 1999). Both strains were crossed to obtain *Brca1f11/f11;p53fp/fp* mice. *p53fp/fp* or *Brca1f11/f11;p53fp/fp* mice were crossed with *Wap-Cre* mice and genotyped to obtain the $p53^{\Delta5-6/\Delta5-6}$ or $Brca1^{\Delta11/\Delta11}$; $p53^{\Delta5-6/\Delta5-6}$ strain, respectively. Dissected mouse mammary tumors were fixed in 4% paraformaldehyde overnight. Sections (4–5 μm) were deparaffinized, hydrated, and digested in 0.05% trypsin at 37°C. After being blocked with 3% H_2O_2 and nonimmune horse serum, sections were incubated at room temperature with a rabbit anti-mouse CD31 antibody and link antibodies, followed by peroxidase-conjugated streptavidin complex and diaminobenzidine tetrahydroxychloride solution as the peroxidase substrate (Vector Laboratories). The sections were counterstained with hematoxylin. Photomicrographs were taken with Zeiss Axioplan 2 Imaging platform and AxioVision 4.4 Software. Six to eight nonoverlapping images for each tumor sample were captured at 200× magnification and analyzed for vascular pathology using AxioVion 4.4. Briefly, each blood vessel was marked and the number within a field of 200× magnification was counted. The lumen of an individual vessel was outlined to compute the area, and the total luminal area of the field was determined. The mean luminal area of a single vessel within a field was calculated and then averaged among multiple fields for each tumor sample. The statistical significance was evaluated by Student's t test using MS Excel XP. High-magnification images were captured at 1000× magnification.

Supplemental data

The Supplemental Data include one supplemental figure and one supplemental table and can be found with this article online at http://www.cancercell.org/cgi/content/full/10/1/13/DC1/.

Acknowledgments

We thank Dr. Peter Oettgen (Harvard Institutes of Medicine, MA) for *ANG1* reporter constructs; Dr. Christopher Hughes (UCI) for HUVECs; Dr. Takahiro Nagase (Kazusa DNA Research Institute, Chiba, Japan) for the KIAA0003 clone; Dr. Chu-Xia Deng (NIH) for *Brca1*-floxed mice; and Eric Wang, Christopher Smith, and Suh-Chin J. Lin for their assistance. This work was supported by grants from the National Institutes of Health (RO1 CA94170 to W.-H.L.; R37 CA049649 to E.Y.-H.P.L.), a predoctoral fellowship from the Department of Defense (W81XWH-05-1-0322 to S.F.), and a physician scientist award from the National Health Research Institute in Taiwan to Y.-M.J.

Received: December 1, 2005
Revised: March 18, 2006
Accepted: May 2, 2006
Published: July 17, 2006

References

Brown, C., Gaspar, J., Pettit, A., Lee, R., Gu, X., Wang, H., Manning, C., Voland, C., Goldring, S.R., Goldring, M.B., et al. (2004). ESE-1 is a novel transcriptional mediator of angiopoietin-1 expression in the setting of inflammation. J. Biol. Chem. *279*, 12794–12803.

Caine, G.J., Blann, A.D., Stonelake, P.S., Ryan, P., and Lip, G.Y.H. (2003). Plasma angiopoietin-1, angiopoietin-2 and Tie-2 in breast and prostate cancer: a comparison with VEGF and Flt-1. Eur. J. Clin. Invest. *33*, 883–890.

Chen, Y., Chen, C.F., Riley, D.J., Allred, D.C., Chen, P.L., Von Hoff, D., Osborne, C.K., and Lee, W.H. (1995). Aberrant subcellular localization of BRCA1 in breast cancer. Science *270*, 789–791.

Chen, Y., Farmer, A.A., Chen, C.F., Jones, D.C., Chen, P.L., and Lee, W.H. (1996). BRCA1 is a 220-kDa nuclear phosphoprotein that is expressed and phosphorylated in a cell cycle-dependent manner. Cancer Res. *56*, 3168–3172.

Chen, P.L., Liu, F., Cai, S., Lin, X., Li, A., Chen, Y., Gu, B., Lee, E.-H.P., and Lee, W.-H. (2005). Inactivation of CtIP leads to early embryonic lethality mediated by G1 restraint and to tumorigenesis by haploid insufficiency. Mol. Cell. Biol. *25*, 3535–3542.

Chinnadurai, G. (2006). CtIP, a candidate tumor susceptibility gene is a team player with luminaries. Biochim. Biophys. Acta *1765*, 67–73.

Couch, F.J., DeShano, M.L., Blackwood, M.A., Calzone, K., Stopfer, J., Campeau, L., Ganguly, A., Rebbeck, T., and Weber, B.L. (1997). BRCA1 mutations in women attending clinics that evaluate the risk of breast cancer. N. Engl. J. Med. *336*, 1409–1415.

Cullmann, G., Fien, K., Kobayashi, R., and Stillman, B. (1995). Characterization of the five replication factor C genes of Saccharomyces cerevisiae. Mol. Cell. Biol. *15*, 4661–4671.

Davila, M., Frost, A.R., Grizzle, W.E., and Chakrabarti, R. (2003). LIM kinase 1 is essential for the invasive growth of prostate epithelial cells: implications in prostate cancer. J. Biol. Chem. *278*, 36868–36875.

Debnath, J., Muthuswamy, S.K., and Brugge, J.S. (2003). Morphogenesis and oncogenesis of MCF-10A mammary epithelial acini grown in three-dimensional basement membrane cultures. Methods *30*, 256–268.

Easton, D.F., Bishop, D.T., Ford, D., and Crockford, G.P. (1993). Genetic linkage analysis in familial breast and ovarian cancer: results from 214 families. The Breast Cancer Linkage Consortium. Am. J. Hum. Genet. *52*, 678–701.

Foulkes, W.D., Metcalfe, K., Hanna, W., Lynch, H.T., Ghadirian, P., Tunng, N., Olopade, O., Weber, B.L., McLennan, J., Olivotto, I.A., et al. (2003). Disruption of the expected positive correlation between breast tumor size and lymph node status in BRCA1-related breast carcinoma. Cancer *98*, 1569–1577.

Furuta, S., Jiang, X., Gu, B., Cheng, E., Chen, P.L., and Lee, W.H. (2005). Depletion of BRCA1 impairs differentiation but enhances proliferation of mammary epithelial cells. Proc. Natl. Acad. Sci. USA *102*, 9176–9181.

Fusco, C., Reymond, A., and Zervos, A.S. (1998). Molecular cloning and characterization of a novel retinoblastoma-binding protein. Genomics *51*, 351–358.

Goffin, J.R., Straume, O., Chappuis, P.O., Brunet, J.-S., Bégin, L.R., Hamel, N., Wong, N., Akslen, L.A., and Foulkes, W.D. (2003). Glomeruloid microvascular proliferation is associated with p53 expression, germline BRCA1 mutations and an adverse outcome following breast cancer. Br. J. Cancer *89*, 1031–1034.

Hakem, R., de la Pompa, J.L., Sirard, C., Mo, R., Woo, M., Hakem, A., Wakeham, A., Potter, J., Reitmair, A., Billia, F., et al. (1996). The tumor suppressor gene Brca1 is required for embryonic cellular proliferation in the mouse. Cell *85*, 1009–1023.

Hashizume, R., Fukuda, M., Maeda, I., Nishikawa, H., Oyake, D., Yabuki, Y., Ogata, H., and Ohta, T. (2001). The RING heterodimer BRCA1-BARD1 is a ubiquitin ligase inactivated by a breast cancer-derived mutation. J. Biol. Chem. *276*, 14537–14540.

Hayes, A.J., Huang, W.Q., Mallah, J., Yang, D., Lippman, M.E., and Li, L.Y. (1999). Angiopoietin-1 and its receptor Tie-2 participate in the regulation of capillary-like tubule formation and survival of endothelial cells. Microvasc. Res. *58*, 224–237.

He, T.-C., Zhou, S., da Costa, L.T., Yu, J., Kinzler, K.W., and Vogelstein, B. (1998). A simplified system for generating recombinant adenoviruses. Proc. Natl. Acad. Sci. USA *95*, 2509–2514.

Imura, S., Miyake, H., Izumi, K., Iashiro, S., and Uehara, H. (2004). Correlation of vascular endothelial cell proliferation with microvessel density and expression of vascular endothelial growth factor and basic fibroblast growth factor in hepatocellular carcinoma. J. Med. Invest. *51*, 202–209.

Kwak, H.J., So, J.N., Lee, S.J., Kim, I., and Koh, G.Y. (1999). Angiopoietin-1 is an apoptosis survival factor for endothelial cells. FEBS Lett. *448*, 249–253.

Lane, T.F., Deng, C., Elson, A., Lyu, M.S., Kozak, C.A., and Leder, P. (1995). Expression of Brca1 is associated with terminal differentiation of ectodermally and mesodermally derived tissues in mice. Genes Dev. *9*, 2712–2722.

Li, S., Chen, P.L., Subramanian, T., Chinnadurai, G., Tomlinson, G., Osborne, C.K., Sharp, Z.D., and Lee, W.-H. (1999). Binding of CtIP to the BRCT repeats of BRCA1 involved in the transcription regulation of p21 is disrupted upon DNA damage. J. Biol. Chem. *274*, 11334–11338.

Li, S., Ting, N.S.Y., Zheng, L., Chen, P.L., Zlv, Y., Shlloh, Y., Lee, E.-H.P., and Lee, W.-H. (2001). Functional link of BRCA1 and ataxia telangiectasia gene product in DNA damage response. Nature *406*, 210–215.

Lin, S.C., Lee, K.F., Nikitin, A.Y., Hilsenbeck, S.G., Cardiff, R.D., Li, A., Kang, K.W., Frank, S.A., Lee, W.-H., and Lee, E.Y. (2004). Somatic mutation of p53 leads to estrogen receptor alpha-positive and -negative mouse mammary tumors with high frequency of metastasis. Cancer Res. *64*, 3525–3532.

Liu, C.Y., Flesken-Nikitin, A., Li, S., Zeng, Y., and Lee, W.H. (1996). Inactivation of the mouse Brca1 gene leads to failure in the morphogenesis of the egg cylinder in early postimplantation development. Genes Dev. *10*, 1835–1843.

Machein, M.R., Knedla, A., Knoth, R., Wagner, S., Neuschl, E., and Plate, K.H. (2004). Angiopoietin-1 promotes tumor angiogenesis in a rat glioma model. Am. J. Pathol. *165*, 1557–1570.

Marquis, S.T., Rajan, J.V., Wynshaw-Boris, A., Xu, J., Yin, G.Y., Abel, K.J., Weber, B.L., and Chodosh, L.A. (1995). The developmental pattern of Brca1 expression implies a role in differentiation of the breast and other tissues. Nat. Genet. *11*, 17–26.

Miki, Y., Swensen, J., Shattuck-Eidens, D., Futreal, P.A., Harshman, K., Tavtigian, S., Liu, Q., Cochran, C., Bennett, L.M., and Ding, W. (1994). A strong candidate for the breast and ovarian cancer susceptibility gene BRCA1. Science *266*, 66–71.

Nomura, N., Miyajima, N., Sazuka, T., Tanaka, A., Kawarabayasi, Y., Sato, S., Nagase, T., Seki, N., Ishikawa, K., and Tabata, S. (1994). Prediction of the coding sequences of unidentified human genes. DNA Res. *1*, 27–35.

Saccani, S., Pantano, S., and Natoli, G. (2001). Two waves of nuclear factor B recruitment to target promoters. J. Exp. Med. *193*, 1351–1359.

Schaeper, U., Subramanian, T., Lim, L., Boyd, J.M., and Chinnadurai, G. (1998). Interaction between a cellular protein that binds to the C-terminal region of adenovirus E1A (CtBP) and a novel cellular protein is disrupted by E1A through a conserved PLDLS motif. J. Biol. Chem. *273*, 8549–8552.

Shekhar, M.P.V., Werdell, J., and Tait, L. (2000). Interaction with endothelial cells is a prerequisite for branching ductal-alveolar morphogenesis and hyperplasia of preneoplastic human breast epithelial cells: regulation by estrogen. Cancer Res. *60*, 439–449.

Stoppa-Lyonnet, D., Ansquer, Y., Dreyfus, H., Gautier, C., Gauthier-Villars, M., Bourstyn, E., Clough, K.B., Magdelenat, H., Pouillart, P., Vincent-Salomon, A., et al. (2000). Familial invasive breast cancers: worse outcome related to BRCA1 mutations. J. Clin. Oncol. *18*, 4053–4059.

Sui, G., Soohoo, C., Affar el, B., Gay, F., Shi, Y., Forrester, W.C., and Shi, Y. (2002). A DNA vector-based RNAi technology to suppress gene expression in mammalian cells. Proc. Natl. Acad. Sci. USA *99*, 5515–5520.

Suri, C., Jones, P.F., Patan, S., Bartunkova, S., Maisonpierre, P.C., Davis, S., Sato, T.N., and Yancopoulos, G.D. (1996). Requisite role of angiopoietin-1, a ligand for the TIE2 receptor, during embryonic angiogenesis. Cell *87*, 1171–1180.

Takakura, N., Watanabe, T., Suenobu, S., Yamada, Y., Noda, T., Ito, Y., Satake, M., and Suda, T. (2000). A role for hematopoietic stem cells in promoting angiogenesis. Cell *102*, 199–209.

Tan, W., Zheng, L., Lee, W.H., and Boyer, T.G. (2004). Functional dissection of transcription factor ZBRK1 reveals zinc fingers with dual roles in DNA-binding and BRCA1-dependent transcriptional repression. J. Biol. Chem. *279*, 6576–6587.

Tessari, M.A., Gostissa, M., Altamura, S., Sgarra, R., Rustighi, A., Salvagno, C., Caretti, G., Imbriano, C., Mantovani, R., Del Sal, G., et al. (2003). Transcriptional activation of the cyclin A gene by the architectural transcription factor HMGA2. Mol. Cell. Biol. *23*, 9104–9116.

Thompson, M.E., Jensen, R.A., Obermiller, P.S., Page, D.L., and Holt, J.T. (1995). Decreased expression of BRCA1 accelerates growth and is often present during sporadic breast cancer progression. Nat. Genet. *9*, 444–450.

Thurston, G., Wang, Q., Baffert, F., Rudge, J., Papadopoulos, N., Jean-Guillaume, D., Wiegand, S., Yancopoulos, G.D., and McDonald, D.M. (2005). Angiopoietin 1 causes vessel enlargement, without angiogenic sprouting, during a critical developmental period. Development *132*, 3317–3326.

Xu, X., Wagner, K.U., Larson, D., Weaver, Z., Li, C., Ried, T., Hennighausen, L., Wynshaw-Boris, A., and Deng, C.X. (1999). Conditional mutation of Brca1 in mammary epithelial cells results in blunted ductal morphogenesis and tumour formation. Nat. Genet. *22*, 37–43.

Yu, X., and Chen, J. (2004). DNA damage-induced cell cycle checkpoint control requires CtIP, a phosphorylation-dependent binding partner of BRCA1 C-terminal domains. Mol. Cell. Biol. *24*, 9478–9486.

Yu, X., Wu, L.C., Bowcock, A.M., Aronheim, A., and Baer, R. (1998). The C-terminal (BRCT) domains of BRCA1 interact in vivo with CtIP, a protein implicated in the CtBP pathway of transcriptional repression. J. Biol. Chem. *273*, 25388–25392.

Zheng, L., Li, S., Boyer, T.G., and Lee, W.-H. (2000a). Lessons learned from BRCA1 and BRCA2. Oncogene *19*, 6159–6175.

Zheng, L., Pan, H., Li, S., Flesken-Nikitin, A., Chen, P.L., Boyer, T.G., and Lee, W.H. (2000b). Sequence-specific transcriptional corepressor function for BRCA1 through a novel zinc finger protein, ZBRK1. Mol. Cell *6*, 757–768.

Zhong, Q., Chen, C.F., Li, S., Chen, Y., Wang, C.C., Xiao, J., Chen, P.L., Sharp, Z.D., and Lee, W.H. (1999). Association of BRCA1 with the hRad50-hMre11-p95 complex and the DNA damage response. Science *285*, 747–750.

Accession numbers

Microarray data are available at Gene Expression Omnibus (GEO; http://www.ncbi.nlm.nih.gov/geo/) with the following accession numbers: BRCA1-KD (GSM106933, GSM106968) versus Luc-KD (GSM106971, GSM106972); and CtIP-KD (GSM106974, GSM106975) versus Luc-KD (GSM106976, GSM106977).